8348 *Macromolecules* **2010**, *43*, 8348–8352
DOI: 10.1021/ma1018445

Macromolecules
COMMUNICATION TO THE EDITOR

Isoindigo-Based Donor−Acceptor Conjugated Polymers

Romain Stalder, Jianguo Mei, and John R. Reynolds*

The George and Josephine Butler Polymer Research Laboratory, Department of Chemistry and Center for Macromolecular Science and Engineering, University of Florida, Gainesville, Florida 32611-7200

Received August 11, 2010
Revised Manuscript Received September 1, 2010

Introduction. The creativity of synthetic chemists working in the field of organic electronics has led to a wealth of functional conjugated organic materials, among which conjugated polymers play a prominent role. The past decade has seen the rapid development of donor−acceptor systems, which have proven efficient at tuning the HOMO and LUMO levels of organic semiconductors, let alone their band gaps.[1,2] Although acceptors such as benzothiadiazole and related derivatives have become popular and are still the focus of intensive research, the rational design of new donor−acceptor systems remains of synthetic interest. Prompted by the need for electron-conducting organic materials, the arylene imide family of acceptors, led by perylene diimide (PDI), has been extensively studied: PDI as a small molecule shows high n-type mobility (> 1 cm^2/V·s) in air-stable organic field effect transistors[3−10] (OFETs). Its dibromo derivative was recently polymerized with electron rich units affording conjugated polymers with propensity for either accepting electrons in all-polymer solar cells[11−13] or conducting electrons in n-type OFETs.[14] With less extended conjugation, naphthalene diimide (NDI) also shows high n-type mobility in small molecule[7,15−19] or polymer[14,20] OFETs. Unfortunately, the 2,6 dibromination[21] and 2,3,6,7 tetrabromination[22] of NDI precursors are harsh, in fuming sulfuric acid at 85 °C or higher. Similarly strong conditions are required for the bromination of PDI, for which the separation of the (minor) 1,6 and (major) 1,7 dibrominated isomers remains an additional issue.[14,23] Recently reported acceptors include 2,2′-bithiophene-3,3′-dicarboximide,[24] pyromellitic diimide,[25] and thieno[3,4-*c*]pyrrole-4,6(5*H*)-dione.[26−28] While 2,2′-bithiophene-3,3′-dicarboximide-based polymers perform well in OFETs—both n-channel and p-channel depending on the nature of the comonomer, conversion from the arylene anhydride to the diimide is not trivial as it was only successfully carried out using microwave irradiation at 220 °C. Thieno[3,4-*c*]pyrrole-4,6(5*H*)-dione is the most promising latest diimide acceptor for donor−acceptor polymers in BHJ solar cells, yet its dibromination is low-yielding and requires a heated concentrated sulfuric acid solution using dibromocyanuric acid as a bromination reagent. For all diimides, the alkyl group is preinstalled on the amine and thus present as the imide condensation takes place, often in low yields which hinders the study of *N*-alkyl substitution effects.

In the past few years, small molecules[29,30] and polymers[31−37] incorporating the diketopyrrolopyrrole (DPP) unit have been reported, along with some of the best performances as p-type materials in conjunction with the n-type fullerenes for organic solar cells: power conversion efficiencies of 4.7% were achieved for DPP-based polymer/PCBM cells and 4.4% for the DPP-based small molecule alternatives. Both centrosymmetric ketopyrrole-containing cores, DPP and isoindigo can undergo facile base-mediated alkylations, which is an attractive synthetic feature since device performance is often influenced by the nature of the alkyl side-chains. Inspired by the latest work on DPP oligomers for organic solar cells, we recently reported the use of isoindigo—synthesized from commercially available precursors in high yields—as an efficient acceptor in donor−acceptor p-type oligomers for bulk heterojunction solar cells.[38] In this communication, we present the synthesis of the first set of isoindigo-based donor−acceptor conjugated polymers and their optical and electrochemical properties. The LUMO levels of such materials are comparable to those of DPP-based polymers, as determined by cyclic voltammetry (CV) and differential pulse voltammetry (DPV), while the HOMO levels are generally deeper for the isoindigo-based conjugated polymers. Still, with band gaps between 1.77 and 1.99 eV, their solid state absorption spectra span the entire visible range; the combination of which with deep energy levels makes these new donor−acceptor conjugated polymers strong candidates for all-polymer solar cells.

Results and Discussion. *Polymer Synthesis and Characterization.* Six representative isoindigo-based conjugated polymers were synthesized by the palladium-catalyzed polycondensations of 6,6′-dibromoisoindigo compound **4** with functionalized electron-rich moieties, as depicted in Scheme 1. The synthesis of **4**, reported in our previous work,[38] was carried out in two high yielding steps from the commercially available 6-bromooxindole (**1**) and 6-bromoisatin (**2**). The borylations of 3,4-dioctylthiophene,[39] 1,4-bis(hexyloxy)benzene,[40] and 9,9-dihexylfluorene[41] were performed according to previously reported procedures. The distannyl compounds were purchased or prepared by direct lithiation with *n*-butyllithium followed by quenching with trimethyltin chloride. The polycondensations were carried out under Stille or Suzuki coupling conditions depending on the nature of the electron-rich comonomer, using $Pd_2(dba)_3$ as a catalyst and $P(o\text{-tyl})_3$ as the corresponding ligand. In particular, the use of ortho substituted triaryl phosphines such as tri-*o*-tolylphosphine ligands have been reported to decrease the polymerization time and increase the molecular weights of afforded polymers.[42] A 20 wt % degassed aqueous solution of Et_4NOH was selected as an organic base for the Suzuki polycondensations.[31,38,39,43] The polymerizations were carried out at 85 °C for 36 h in degassed toluene/water mixture, where both the activated boronate salts and the resulting polymers are soluble.

The polymers were collected by filtration after precipitation into methanol and purified by Soxhlet extraction using methanol, hexanes, and chloroform fractions. The fractionation yields vary depending on the solubility of the material: for **P2**, **P3**, and **P6**, both the hexanes and the chloroform fractions contained significant amounts of polymer (see Supporting Information for exact yields), while only the chloroform fraction of **P1** contained significant amounts of material. After evaporation of the solvent, **P1** shows considerable mechanical strength. Figure 1a shows a 20 cm-diameter free-standing film of **P1** peeled off of a glass Petri dish after

---

*Corresponding author. E-mail: reynolds@chem.ufl.edu.

Scheme 1. Synthesis of Monomer 4 and the Polymer Set P1 through P6

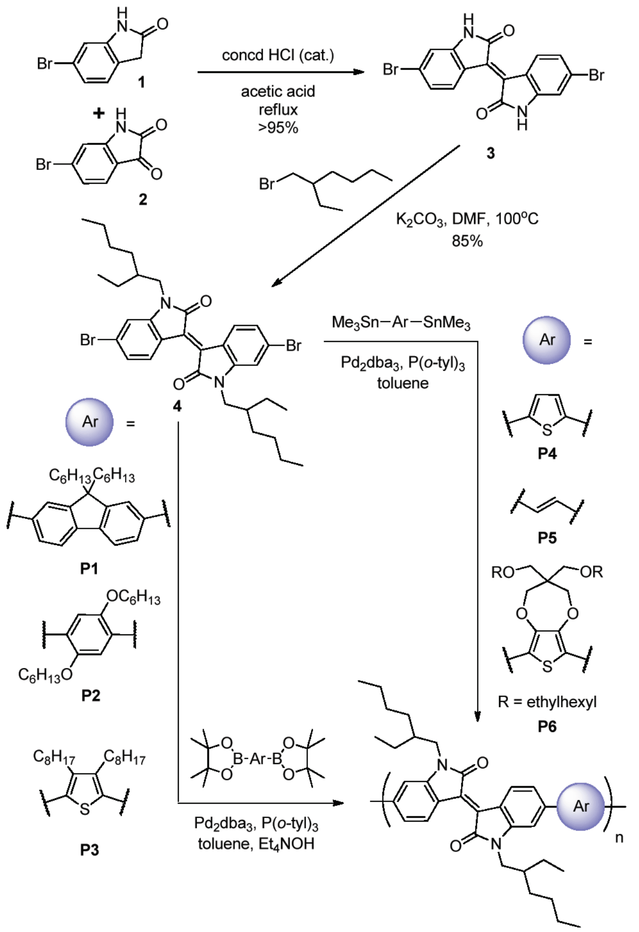

evaporation of the solvent. The lack of alkyl chains on the thiophene and vinyl units of **P4** and **P5** leads to low solubility and limited yields after extraction from chloroform. The remainder of this study was carried out on samples out of the chloroform fractions, which contain the higher molecular weights. Estimation of these molecular weights against polystyrene standards using size exclusion chromatography (SEC) with THF as eluent gives number-average molecular weights (M_n) within 10−22 kDa for the polymers bearing alkyl chains on the donor unit, while the recorded M_n for **P4** and **P5** suffered from poor solubility in THF for SEC analysis and possibly in the toluene reaction medium, leading to M_n of 2.4 and 1.9 kDa for **P4** and **P5** respectively.

The proton NMR spectra of all polymers show broad peaks in the 6.5−9.4 ppm range corresponding to the aromatic protons, as well as broad multiplets in the 0.70−1.80 ppm corresponding to the alkyl chain protons other than the ones on the tertiary carbon of the branched chains (around 1.90 ppm) and the ones on the carbon next to the isoindigo nitrogen (in the 3.50−3.90 ppm range). A representative ^{1}H NMR spectrum of the polymer set is shown for **P1** in Figure 1b. While **P4** and **P5** show no other alkyl chain peaks as expected, additional broad peaks in the 3.65−3.85 ppm range (alkyl protons next to the oxygen) for **P2**, in the 2.50−3.05 ppm range (alkyl protons next to the thiophene ring) for **P3** and centered at 4.20 pm, 3.60 and 3.30 ppm (alkyl protons next to oxygens) for **P6** are consistent with the chemical structure of the repeat unit of each polymer.

Thermogravimetric analysis (TGA) under nitrogen flow was used to evaluate the thermal stability of the purified polymers. A mass loss of 5% is defined as the threshold for thermal decomposition. All materials demonstrate good thermal stability with decomposition temperatures above 325 °C. We employed differential scanning calorimetry to investigate any phase transitions in the materials, but no significant transitions were observed. The thermal data and the SEC results are summarized in Table 1.

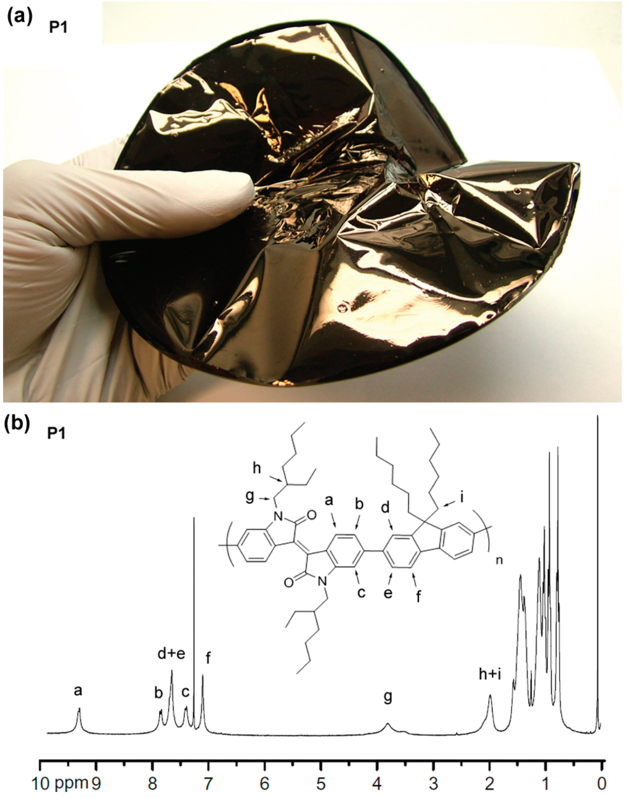

Figure 1. (a) A 20 cm-diameter free-standing film of **P1** and (b) ^{1}H NMR spectrum of **P1** in $CDCl_3$.

Electrochemical Characterization. Cyclic voltammetry (CV) and differential pulse voltammetry (DPV) experiments were carried out on thin films of each polymer to evaluate their redox properties (HOMO and LUMO energy levels). Representative CV and DPV of **P4** are displayed in Figure 2 and the corresponding voltammograms of the other five polymers are included in the Supporting Information.

P4 shows a quasi-reversible oxidation, with a half-wave potential ($E_{1/2}^{ox}$) located at 0.91 V versus Fc/Fc$^+$ and two quasi-reversible reductions with $E_{1/2}^{red}$ located at −1.24 V and −1.62 V versus Fc/Fc$^+$. While the generation of the anion radical during the first reduction process at $E_{1/2}^{red}$ = −1.24 V is stable to repeated cycles, the second reduction process was unstable under the selected electrochemical conditions. The overall CV data for the six polymers is summarized in Table 1. The HOMO and LUMO energy levels can be calculated from the onsets of oxidation and reduction, respectively, with Fc/Fc$^+$ set at −5.1 V.[44] DPV usually allows to record voltammograms with sharper oxidation and reduction onsets, so we chose to record the onsets of oxidation (E_{on}^{ox}) and reduction (E_{on}^{red}) from the solid state DPV data displayed in Figure 2 for **P4** and in the Supporting Information for the other polymers, and also summarized in Table 1. The LUMO levels are found over a narrow range: the LUMO for **P4** is the deepest at −3.95 eV, while **P1** has the highest at −3.84 eV; these levels approach the LUMOs of PCBM derivatives. The DPP-based analogues of **P1** and **P4** reported in the literature have similar LUMO levels, measured at −3.87 eV for DPP-*co*-thiophene

Table 1. Molecular Weights and Polydispersities[a], Thermal Stability, Optical Properties, and Electrochemical Data for Polymers P1–P6

							electrochemistry[d]				
				UV–vis–NIR			CV		DPV		
	M_n[a] (kDa)	M_w/M_n	T_d (°C)	λ_{max}[b] (nm)	λ_{max}[c] (nm)	E_{gap}^{optc} (eV)	$E_{1/2}^{ox}$ (V)	$E_{1/2}^{red}$ (V)	E_{on}^{ox} (V)/ HOMO(eV)	E_{on}^{red} (V)/ LUMO(eV)	E_{gap} (eV)
P1	21.2	1.96	390	564	561	1.87	1.01	−1.17	0.73/−5.83	−1.26/−3.84	1.99
P2	10.5	2.13	371	555	573	1.75	0.90	−1.34	0.70/−5.80	−1.23/−3.87	1.93
P3	16.7	1.94	377	609	633	1.79	1.02	−1.30	0.64/−5.74	−1.25/−3.85	1.89
P4	2.4	1.13	359	647	604	1.60	0.91	−1.24	0.71/−5.81	−1.15/−3.95	1.86
P5	1.9	1.20	340	612	640	1.66		−1.18	0.66/−5.76	−1.17/−3.93	1.83
P6	19.3	1.70	367	701	710	1.55	0.75	−1.21	0.58/−5.68	−1.19/−3.91	1.77

[a] Determined by SEC in THF against polystyrene standards; **P4** and **P5** only slightly soluble in THF. [b] In chloroform solution. [c] Recorded for thin films spayed onto ITO-coated glass. [d] Recorded for thin films drop-cast from toluene onto Pt button electrodes.

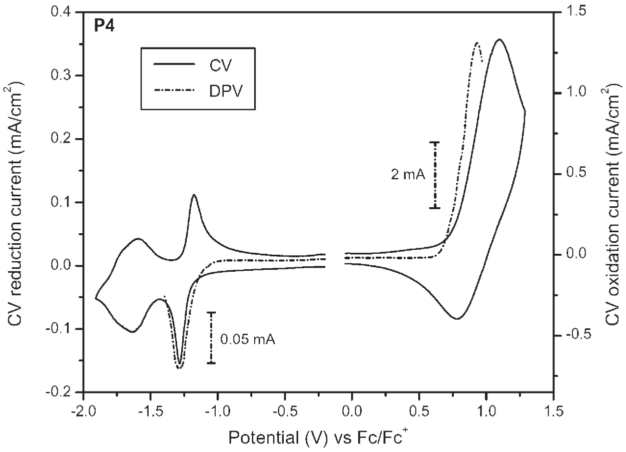

Figure 2. Cyclic voltammogram and differential pulse voltammogram of a **P4** thin film on Pt-button electrode, recorded at a 50 mV/s scan rate in 0.1 M (TBA)PF$_6$ acetonitrile solution.

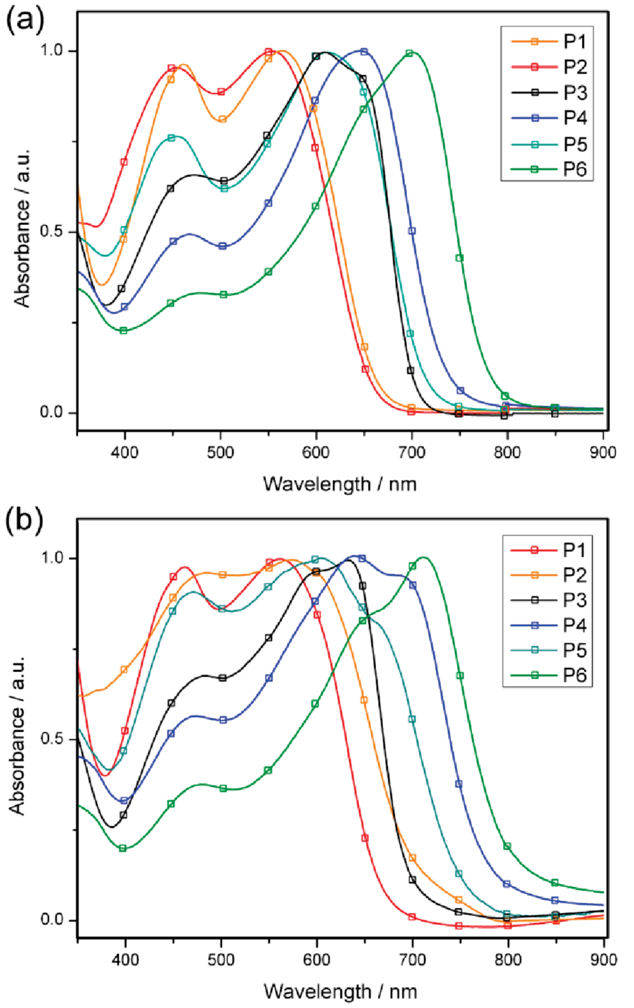

Figure 3. Normalized UV–vis absorption spectra of **P1** through **P6**: (a) in chloroform solution; (b) as thin films on ITO-coated glass.

and at −3.85 eV for DPP-*co*-fluorene polymers.[36] The HOMO levels of isoindigo-based polymers are spread between −5.68 and −5.83 eV, which is at least 0.3 eV deeper than those of DPP-*co*-fluorene and DPP-*co*-thiophene polymers,[36] and generally deeper than those of the best performing n-type polymers in all-polymer devices reported so far[12,45−51] Electrochemical band gaps were calculated to be within 1.77 to 1.99 eV (Table 1). Such deep HOMOs are adequate for isoindigo-based polymers to form type II heterojunctions with common electron-donating polymers such as P3HT or MEH-PPV.[52]

Optical Properties. The UV–vis spectrum of each polymer in solution displays two absorption bands characteristic of donor–acceptor systems:[53,54] a high-energy band located in the 420–490 nm range attributed to the $\pi-\pi^*$ transition, and a low-energy band in the 520–800 nm range assigned to intramolecular charge transfer. As depicted in Figure 3a, polymers **P1** and **P2** have similar absorption spectra in solution with high-energy peaks at 462 and 452 nm respectively, and low-energy peaks at 564 and 555 nm, respectively. For **P1** and **P2**, the relative intensities of these two bands are comparable and are close to unity.

With red-shifted absorption maxima, the peaks for **P3** are located at 472 and 609 nm, with a decreased intensity of the high-energy band relative to the low-energy band. The spectrum for **P5** is similar to **P3** with peaks at 454 and 612 nm. The trend on going from **P1** or **P2** to **P3** is accentuated for **P4** and even further for **P6**: Figure 3a shows bathochromic shifts of 35 and 89 nm for the low-energy absorption maxima of **P4** and **P6** respectively compared to **P3**. The intensities of their high-energy bands decrease further relative to their low-energy bands, to a point where little absorption remains at high energy (below 500 nm) for **P6** in solution. While the variations in relative intensities of the high- and low-energy bands would require deeper analysis in order to definitely relate polymer structure and absorption profile intensities, the trend for chromatic shifts in absorption maxima can be explained by the variations of the electron-donating character of the different electron-rich comonomers to the overall pi-system. Compared to copolymer **P5** containing the vinylene spacer, which we can consider as the simplest conjugated bridge between two consecutive isoindigo moieties, the electron-donating character of the dialkoxybenzene and fluorene spacers is relatively weak. Arguably, these moderately electron-rich units lie out of plane relative to the isoindigo units because of the ortho-hydrogens on the benzene rings, as well as the dialkoxy side chains for **P2**, which could justify the hypsochromic shift of the absorption maxima of **P1** and **P2** compared to **P5**. Although the three thiophene-based spacers of **P3**, **P4**, and **P6** are more electron-rich than the vinylene spacer of **P5**, it is likely that steric hindrance arising from the presence of the dialkyl substituents on the thiophene of **P3** would explain the blue-shift in the UV−vis spectrum of **P3** compared to **P4**. The propylenedioxythiophene spacer of **P6** is the most electron-rich comonomer, resulting in the greatest bathochromic shift. The extinction coefficients of the polymers in solution are summarized in the Supporting Information.

The solid state absorption of the polymer set displayed in Figure 3b was investigated by spraying solutions of the polymers onto ITO-coated glass and recording the thin film absorption spectra. The trend delineated for solution absorption still holds in the solid state, only red-shifted on the order of 10 nm compared to the solution spectra. Interestingly, the absorption of unalkylated **P4** and **P5** broaden significantly compared to the solution absorption, suggesting an enhanced intermolecular interaction of neighboring chains in the solid state for these two polymers. The colors of the polymer thin films are consistent with their absorption profile: **P1** and **P2** films are red-purple due to the broad absorption from 400 nm to ca. 700 nm and little absorption beyond 700 nm. Thin films of **P3** and **P4** have a blue-gray color due to their long-wavelength absorption and the reduced intensity of the low-wavelength absorption band below 550 nm. With long-wavelength absorption even more red-shifted and further reduced low-wavelength absorption, **P6** has a blue-green hue. The broadened absorption of **P5** from 400 to 750 nm in the solid state renders it black to the eye, a much sought after property for applications in the electrochromic and photovoltaic fields of organic materials.[54] Compared to DPP-based analogues, which have low-energy absorption onsets in the 800−1000 nm range in the solid state, the absorption onsets of isoindigo-based polymers are blue-shifted by at least 150 nm depending on the comonomer, which is expected considering their deeper HOMO levels. From these low-energy onsets of absorption in the solid state, optical band gaps in the 1.55−1.90 eV range are estimated (Table 1), which is consistent with the measured electrochemical band gaps and 0.3 to 0.4 eV higher than for DPP-based analogues. Because of this strong absorption in the visible region up to 800 nm—considerably red-shifted compared to the common PCBM (C_{60} and C_{70} derivatives) electron-acceptors, isoindigo-based conjugated polymers could be efficient electron-accepting materials in all-polymer solar cells,[52] especially since their deep HOMO and LUMO levels are suitable for type II heterojunctions with electron-donating polymers.

Conclusions. We designed six donor−acceptor conjugated polymers which, for the first time, copolymerize donors of varying electron-donating strengths with the isoindigo acceptor. Synthesized via Stille or Suzuki polycondensations, these polymers have LUMO levels comprised in the −3.8 to −3.9 eV range, with band gaps between 1.6 and 2.0 eV. The polymers' absorption of light can be tuned throughout the visible region of the spectrum depending on the nature of the electron-rich comonomer, with absorption maxima situated in the 550−710 nm range. The combination of deep HOMO and LUMO levels and tunable absorption extended to 800 nm in the solid state provide isoindigo-based donor−acceptor polymers with attractive properties for photovoltaic applications, which our future work is focusing on.

Acknowledgment. We gratefully acknowledge AFSOR (FA9550-09-1-0320) for financial support. R.S. acknowledges the University Alumni Awards Program for a fellowship.

Supporting Information Available: Text giving synthetic procedures and characterizations, materials, and instrumentation details and figures showing TGA curves, cyclic voltammograms, and differential pulse voltammograms, and a table of molar absorptivities. This material is available free of charge via the Internet at http://pubs.acs.org.

References and Notes

(1) Chen, J. W.; Cao, Y. *Acc. Chem. Res.* **2009**, *42*, 1709–1718.
(2) Cheng, Y. J.; Yang, S. H.; Hsu, C. S. *Chem. Rev.* **2009**, *109*, 5868–5923.
(3) Briseno, A. L.; Mannsfeld, S. C. B.; Reese, C.; Hancock, J. M.; Xiong, Y.; Jenekhe, S. A.; Bao, Z.; Xia, Y. *Nano Lett.* **2007**, *7*, 2847–2853.
(4) Brooks, A. J.; Michael, J. A.; Myung-Han, Y.; Antonio, F.; Tobin, J. M.; Michael, R. W. *Angew. Chem., Int. Ed.* **2004**, *43*, 6363–6366.
(5) Campos, L. M.; Tontcheva, A.; Gunes, S.; Sonmez, G.; Neugebauer, H.; Sariciftci, N. S.; Wudl, F. *Chem. Mater.* **2005**, *17*, 4031–4033.
(6) Chen, H. Z.; Ling, M. M.; Mo, X.; Shi, M. M.; Wang, M.; Bao, Z. *Chem. Mater.* **2007**, *19*, 816–824.
(7) Jones, B. A.; Facchetti, A.; Wasielewski, M. R.; Marks, T. J. *J. Am. Chem. Soc.* **2007**, *129*, 15259–15278.
(8) Oh, J. H.; Liu, S.; Bao, Z.; Schmidt, R.; Wurthner, F. *Appl. Phys. Lett.* **2007**, *91*, 212107.
(9) Schmidt, R.; Ling, M. M.; Oh, J. H.; Winkler, M.; Könemann, M.; Bao, Z.; Würthner, F. *Adv. Mater.* **2007**, *19*, 3692–3695.
(10) Weitz, R. T.; Amsharov, K.; Zschieschang, U.; Villas, E. B.; Goswami, D. K.; Burghard, M.; Dosch, H.; Jansen, M.; Kern, K.; Klauk, H. *J. Am. Chem. Soc.* **2008**, *130*, 4637–4645.
(11) Tan, Z. A.; Zhou, E. J.; Zhan, X. W.; Wang, X.; Li, Y. F.; Barlow, S.; Marder, S. R. *Appl. Phys. Lett.* **2008**, *93*, 073309.
(12) Zhan, X. W.; Tan, Z. A.; Domercq, B.; An, Z. S.; Zhang, X.; Barlow, S.; Li, Y. F.; Zhu, D. B.; Kippelen, B.; Marder, S. R. *J. Am. Chem. Soc.* **2007**, *129*, 7246–7247.
(13) Zhan, X. W.; Tan, Z. A.; Zhou, E. J.; Li, Y. F.; Misra, R.; Grant, A.; Domercq, B.; Zhang, X. H.; An, Z. S.; Zhang, X.; Barlow, S.; Kippelen, B.; Marder, S. R. *J. Mater. Chem.* **2009**, *19*, 5794–5803.
(14) Chen, Z.; Zheng, Y.; Yan, H.; Facchetti, A. *J. Am. Chem. Soc.* **2008**, *131*, 8–9.
(15) Katz, H. E.; Johnson, J.; Lovinger, A. J.; Li, W. J. *J. Am. Chem. Soc.* **2000**, *122*, 7787–7792.
(16) Katz, H. E.; Lovinger, A. J.; Johnson, J.; Kloc, C.; Siegrist, T.; Li, W.; Lin, Y. Y.; Dodabalapur, A. *Nature* **2000**, *404*, 478–481.
(17) Lee, Y. L.; Hsu, H. L.; Chen, S. Y.; Yew, T. R. *J. Phys. Chem. C* **2008**, *112*, 1694–1699.
(18) See, K. C.; Landis, C.; Sarjeant, A.; Katz, H. E. *Chem. Mater.* **2008**, *20*, 3609–3616.
(19) Shukla, D.; Nelson, S. F.; Freeman, D. C.; Rajeswaran, M.; Ahearn, W. G.; Meyer, D. M.; Carey, J. T. *Chem. Mater.* **2008**, *20*, 7486–7491.
(20) Yan, H.; Chen, Z.; Zheng, Y.; Newman, C.; Quinn, J. R.; Dotz, F.; Kastler, M.; Facchetti, A. *Nature* **2009**, *457*, 679–686.
(21) Chaignon, F.; Falkenstrom, M.; Karlsson, S.; Blart, E.; Odobel, F.; Hammarstrom, L. *Chem. Commun.* **2007**, 64–66.
(22) Gao, X. K.; Qiu, W. F.; Yang, X. D.; Liu, Y. Q.; Wang, Y.; Zhang, H. J.; Qi, T.; Liu, Y.; Lu, K.; Du, C. Y.; Shuai, Z. G.; Yu, G.; Zhu, D. B. *Org. Lett.* **2007**, *9*, 3917–3920.
(23) Wurthner, F.; Stepanenko, V.; Chen, Z.; Saha-Moller, C. R.; Kocher, N.; Stalke, D. *J. Org. Chem.* **2004**, *69*, 7933–7939.
(24) Letizia, J. A.; Salata, M. R.; Tribout, C. M.; Facchetti, A.; Ratner, M. A.; Marks, T. J. *J. Am. Chem. Soc.* **2008**, *130*, 9679–9694.
(25) Zheng, Q. D.; Huang, J.; Sarjeant, A.; Katz, H. E. *J. Am. Chem. Soc.* **2008**, *130*, 14410–14411.
(26) Piliego, C.; Holcombe, T. W.; Douglas, J. D.; Woo, C. H.; Beaujuge, P. M.; Frechet, J. M. J. *J. Am. Chem. Soc.* **2010**, *132*, 7595–7597.
(27) Zhang, Y.; Hau, S. K.; Yip, H.-L.; Sun, Y.; Acton, O.; Jen, A. K. Y. *Chem. Mater.* **2010**, *22*, 2696–2698.
(28) Zou, Y.; Najari, A.; Berrouard, P.; Beaupres, S.; Aich, R. B.; Tao, Y.; Leclerc, M. *J. Am. Chem. Soc.* **2010**, *132*, 5330–5331.

(29) Tamayo, A. B.; Dang, X. D.; Walker, B.; Seo, J.; Kent, T.; Nguyen, T. Q. *Appl. Phys. Lett.* **2009**, *94*, 3.

(30) Walker, B.; Tomayo, A. B.; Dang, X. D.; Zalar, P.; Seo, J. H.; Garcia, A.; Tantiwiwat, M.; Nguyen, T. Q. *Adv. Funct. Mater.* **2009**, *19*, 3063–3069.

(31) Allard, N.; Aïch, R. B.; Gendron, D.; Boudreault, P.-L. T.; Tessier, C.; Alem, S.; Tse, S.-C.; Tao, Y.; Leclerc, M. *Macromolecules* **2010**, *43*, 2328–2333.

(32) Bijleveld, J. C.; Zoombelt, A. P.; Mathijssen, S. G. J.; Wienk, M. M.; Turbiez, M.; de Leeuw, D. M.; Janssen, R. A. J. *J. Am. Chem. Soc.* **2009**, *131*, 16616–16617.

(33) Huo, L. J.; Hou, J. H.; Chen, H. Y.; Zhang, S. Q.; Jiang, Y.; Chen, T. L.; Yang, Y. *Macromolecules* **2009**, *42*, 6564–6571.

(34) Zhou, E.; Wei, Q.; Yamakawa, S.; Zhang, Y.; Tajima, K.; Yang, C.; Hashimoto, K. *Macromolecules* **2009**, *43*, 821–826.

(35) Zhou, E.; Yamakawa, S.; Tajima, K.; Yang, C.; Hashimoto, K. *Chem. Mater.* **2009**, *21*, 4055–4061.

(36) Zou, Y. P.; Gendron, D.; Neagu-Plesu, R.; Leclerc, M. *Macromolecules* **2009**, *42*, 6361–6365.

(37) Wienk, M. M.; Turbiez, M.; Gilot, J.; Janssen, R. A. J. *Adv. Mater.* **2008**, *20*, 2556–2560.

(38) Mei, J.; Graham, K. R.; Stalder, R.; Reynolds, J. R. *Org. Lett.* **2010**, *12*, 660–663.

(39) Mei, J.; Heston, N. C.; Vasilyeva, S. V.; Reynolds, J. R. *Macromolecules* **2009**, *42*, 1482–1487.

(40) Zhu, Y.; Champion, R. D.; Jenekhe, S. A. *Macromolecules* **2006**, *39*, 8712–8719.

(41) Cho, S. Y.; Grimsdale, A. C.; Jones, D. J.; Watkins, S. E.; Holmes, A. B. *J. Am. Chem. Soc.* **2007**, *129*, 11910–11911.

(42) Towns, C.; Wallace, P.; Allen, I.; Pounds, T.; Murtagh, L. US Patent 20050014926, 2005.

(43) Blouin, N.; Michaud, A.; Leclerc, M. *Adv. Mater.* **2007**, *19*, 2295–2300.

(44) Thompson, B. C.; Kim, Y.-G.; McCarley, T. D.; Reynolds, J. R. *J. Am. Chem. Soc.* **2006**, *128*, 12714–12725.

(45) Holcombe, T. W.; Woo, C. H.; Kavulak, D. F. J.; Thompson, B. C.; Frechet, J. M. J. *J. Am. Chem. Soc.* **2009**, *131*, 14160–14161.

(46) Kietzke, T.; Horhold, H.-H.; Neher, D. *Chem. Mater.* **2005**, *17*, 6532–6537.

(47) Kim, Y.; Cook, S.; Choulis, S. A.; Nelson, J.; Durrant, J. R.; Bradley, D. D. C. *Chem. Mater.* **2004**, *16*, 4812–4818.

(48) Koetse, M. M.; Sweelssen, J.; Hoekerd, K. T.; Schoo, H. F. M.; Veenstra, S. C.; Kroon, J. M.; Yang, X.; Loos, J. *Appl. Phys. Lett.* **2006**, *88*, 083504.

(49) McNeill, C. R.; Abrusci, A.; Zaumseil, J.; Wilson, R.; McKiernan, M. J.; Burroughes, J. H.; Halls, J. J. M.; Greenham, N. C.; Friend, R. H. *Appl. Phys. Lett.* **2007**, *90*, 193506.

(50) McNeill, C. R.; Halls, J. J. M.; Wilson, R.; Whiting, G. L.; Berkebile, S.; Ramsey, M. G.; Friend, R. H.; Greenham, N. C. *Adv. Funct. Mater.* **2008**, *18*, 2309–2321.

(51) Veenstra, S. C.; Verhees, W. J. H.; Kroon, J. M.; Koetse, M. M.; Sweelssen, J.; Bastiaansen, J. J. A. M.; Schoo, H. F. M.; Yang, X.; Alexeev, A.; Loos, J.; Schubert, U. S.; Wienk, M. M. *Chem. Mater.* **2004**, *16*, 2503–2508.

(52) McNeill, C. R.; Greenham, N. C. *Adv. Mater.* **2009**, *21*, 3840–3850.

(53) Amb, C. M.; Beaujuge, P. M.; Reynolds, J. R. *Adv. Mater.* **2009**, *28*, 724–728.

(54) Beaujuge, P. M.; Ellinger, S.; Reynolds, J. R. *Nat. Mater.* **2008**, *7*, 795–799.